Current Research in Food Science 9 (2024) 100911

Contents lists available at ScienceDirect

Current Research in Food Science

journal homepage: www.sciencedirect.com/journal/current-research-in-food-science

Effects of cricket powder on structural and mechanical properties of soy protein isolate extrudates

Zhaojun Wang [a,b], Qian Deng [a,b], Yuliang Zhou [c], Xinyue Qi [c], Leehow Lau [c], Yuqiao He [c], Zhiyong He [a,b], Maomao Zeng [a,b], Qiuming Chen [a,b], Jie Chen [a,b], Hui Ye [c,d,*]

[a] State Key Laboratory of Food Science and Resources, Jiangnan University, Wuxi, 214122, China
[b] School of Food Science and Technology, Jiangnan University, Wuxi, 214122, China
[c] School of Chemistry, Chemical Engineering and Biotechnology, Nanyang Technological University, 637371, Singapore
[d] Singapore Future Ready Food Safety Hub, 50 Nanyang Avenue, N1, B3C-41, 639798, Singapore

ARTICLE INFO

Keywords:
Meat analogs
Cricket powder
Soy protein isolate
High moisture extrusion
Anisotropic structure

ABSTRACT

This study investigated the impact of cricket powder (CP) incorporation on the structural and mechanical properties of soy protein isolate (SPI) extrudates. The physicochemical properties of CP, rheological properties of SPI-CP blends and their potential structuring properties were evaluated. The results showed that CP had a high protein content (72.10 ± 0.61%) and a notable amount of dietary fiber. Rheological analysis revealed that the complex modulus (G^*) of SPI-CP blends decreased over time at 140 °C, with the rate of decrease accelerating with higher CP content. Structural and mechanical analysis indicated that the addition of CP enhanced anisotropic structure formation, with optimal anisotropy observed at 10% CP, while higher concentrations reduced mechanical strength and coherence due to the presence of insoluble components and the formation of large cracks. Flavor analysis showed that CP contributed pyrazines and ethers, imparting a desirable burnt and baked flavor to the extrudates. These findings suggested that CP can be effectively used to improve the textural properties and flavor of SPI-based extrudates at optimal concentrations. However, excessive CP incorporation can compromise structural integrity.

1. Introduction

The rising demand for sustainable protein sources has driven the exploration of alternative ingredients with lower environmental impacts compared to traditional animal proteins. Cricket protein, derived from house crickets (*Acheta domesticus*), is emerging as a sustainable alternative to traditional protein sources. It boasts a significant lower environmental footprint in terms of water usage, land occupation, and greenhouse gas emissions (Gómez et al., 2019; Halloran et al., 2016; Oonincx and De Boer, 2012). The integration of animal with plant-based proteins offers a compelling synergy in food manufacturing, combining the high-quality amino acid profile of animal proteins with the sustainability and dietary fiber benefits of plant proteins (Van Huis, 2013; Xiao et al., 2023). This blend not only enhances nutritional profiles of food products but also contributes to more sustainable food systems by reducing reliance on resource-intensive animal farming.

The combination of plant and animal proteins can address both environmental concerns, and the nutritional deficiencies often associated with purely plant-based diets, offering a balanced solution to future food security and nutritional needs (Alcorta et al., 2021). Cricket protein, in particular, is emerging as a versatile and sustainable ingredient, especially in the development of meat analogs. It offers a rich blend of highly digestible proteins, essential fatty acids, and vital nutrients, including a robust profile of vitamin B complex (Pilco-Romero et al., 2023). Notably, 100 g of dried house cricket can supply over 30% of the Dietary Reference Intake for several nutrients, with some exceeding 100% (Lamsal et al., 2019; Rumpold and Schlüter, 2013).

The functional properties of cricket protein, such as water retention, emulsification, and foaming, are critical for creating textures and flavors akin to those of meat-based products, enhancing the nutritional value and sensory qualities of processed foods (Pilco-Romero et al., 2023; Yi et al., 2013). The integration of cricket protein into various food products not only addresses the increasing consumer demand for sustainable and ethical food choices but also meets current trends towards healthier, protein-rich diets. Its application in meat analogs and cereal-derived products demonstrates its potential to significantly impact food

* Corresponding author. School of Chemistry, Chemical Engineering and Biotechnology, Nanyang Technological University, 637371, Singapore.
E-mail address: ye.hui@ntu.edu.sg (H. Ye).

https://doi.org/10.1016/j.crfs.2024.100911
Received 1 July 2024; Received in revised form 24 October 2024; Accepted 27 October 2024
Available online 31 October 2024

technology (Montowska et al., 2019). With its ability to form gels and emulsions and improve texture, along with ongoing advancements in food processing technology, cricket protein would play a crucial role in the future of food manufacturing, providing innovative solutions to the challenges of dietary sustainability and global food supply (Chirico Scheele et al., 2021).

A recent review summarized three hypotheses governing fiber formation during high moisture extrusion (van der Sman and van der Goot, 2023). The first hypothesis suggests that fiber formation through the alignment of protein (aggregates) in strong shear flow beyond the denaturation temperature (Manski et al., 2007; Wang et al., 2019a). Th e second hypothesis involves two thermodynamically incompatible phases, such as a protein with polysaccharides (e.g., pectin) or a protein with an insoluble protein (e.g., gluten) or fiber (e.g., cellulose), where the dispersed phase is distorted and aligned by flow (Dekkers et al., 2016; Deng et al., 2023; Grabowska et al., 2014; Wang et al., 2019b). The third hypothesis is based on protein-rich and water-rich phase separation (syneresis) leading to anisotropic structure formation (Nieuwland et al., 2023; Wittek et al., 2021). Studies on soy protein isolate (SPI) have shown that an anisotropic structure can be formed through protein-rich and water-rich phase separation only when SPI contains certain amounts of insoluble aggregates (Fu et al., 2023, 2024). Additionally, a second dispersed phase in the SPI continuous phase can enhance fiber formation by promoting fracturing during tearing along the extrusion direction (Deng et al., 2023; Schreuders et al., 2022). Small amounts of fat, low molecular weight saccharides, or proteins can act as plasticizers, improving the fibrous properties and resulting in extrudates with a loose structure (Wang et al., 2023; Xie et al., 2023).

Cricket powder (CP) could serve as a potential protein-rich source to add to SPI, forming two thermodynamically incompatible phases during extrusion. Several studies have demonstrated that CP can be used as an alternative protein source for gluten-free products, such as bread, muffins and cookies(da Rosa Machado and Thys, 2019; Osimani et al., 2018; Pauter et al., 2018; Terry et al., 2017). The addition of cricket protein to plant protein also shows potential for forming fibrous structure through high moisture extrusion. Smetana et al. (2018b, 2019) found that the adding up to 40% of cricket protein concentrate to soy protein concentrate produced optimal meat-like extrudates with the highest inclusion of insect biomass for extrusion at 170 °C. Samuel et al. (Kiiru et al., 2020) obtained fibrous extrudates with the highest anisotropic index of 2.8 at inclusion of 30% low-fat CP. Moreover, the inclusion of CP containing the ideal amount of fat and insoluble fibre may positively affect structure formation (Montowska et al., 2019). Overall, there is limited research on using CP to produce fibrous structures for insect-based meat analogs.

Therefore, the aim of this study was to characterize CP through physicochemical and rheological analyses and to evaluate its effect on SPI-CP extrudates during high moisture extrusion processing. The extrudates were produced using a lab-scale twin-screw extruder with SPI-CP blends containing varying weight ratios of SPI and CP. The structure of the extrudates was examined using confocal laser scanning microscopy (CLSM), and their mechanical properties were measured through tensile testing. The flavor compounds in extrudates were analyzed using GC/O/MS.

2. Materials and methods

2.1. Materials

Cricket powder (CP) was purchased from Darenfucheng Animal Technology Co., Ltd. (Qingdao, China). The powder was prepared after washing, microwave heating (110 °C, ≥10 min) and grinding process according to the manufacturer's specifications. Soy Protein isolate (SPI, SD-100) was purchased from Linyi Shansong Biological Products Co., Ltd. (Shandong, China). The SPI powder contains 83.7 wt% protein (wet base, 65.8 wt% soluble protein), 7.0 wt% moisture, 0.8 wt% fat and 2.0 wt% carbohydrate. Rhodamine B was purchased from J&K Scientific (Beijing, China) and Calcofluor white was purchased from Sigma-Aldrich (Shanghai, China), which were used as the staining agents for protein and cellulose/chitosan for CLSM analysis, respectively. All other chemicals utilized in this study were of analytical grade unless specified otherwise.

2.2. Characterization of CP

The proximate chemical compositions of CP were determined according to Chinese National Standards GB5009.5–2016 GB5009.3–2016, GB5009.6–2016, and GB5009.88–2014 (2016) for the total nitrogen content, moisture, lipid, and dietary fibres, respectively. The total nitrogen content was determined by the Kjeldahl method and was used to calculate the crude protein content by multiplying the result by the conversion factor of 6.25.

Solubility and water holding capacity (WHC) were determined according to the method described by (Fu et al., 2024). The CP dispersion (2.0 wt%) was centrifuged at 10,000 *g* for 30 min at 20 °C. The weight of the wet pellet was measured, and the weight of the freeze-dried pellet was also determined and recorded. The supernatant was collected, and the soluble protein content of the supernatant was determined using the Biuret method. The solubility and WHC were calculated using equation (1), and (2), respectively.

$$Solubility\ (\%) = \frac{M_{dry\ powder} - M_{dry\ pellet}}{M_{dry\ powder}} \times 100 \quad (1)$$

$$Water\ holding\ capacity\ (g/g) = \frac{M_{wet\ pellet} - M_{dry\ pellet}}{M_{dry\ powder}} \quad (2)$$

where $M_{dry\ powder}$ represents the mass of the overall added dry powder, $M_{wet\ pellet}$ is the mass of the pellet after removing supernatant, and $M_{dry\ pellet}$ is the mass of the pellet after centrifugation and freeze-drying.

2.3. Rheological properties

A closed cavity rheometer (RPA Elite, TA Instruments, New Castle, DE) was used to assess the reactions of blends under different thermal and mechanical stresses (Dekkers et al., 2018a,b). The test sample consisted of SPI and CP in weight ratios of 10:0, 9:1, 8:2, 7:3, 6:4, 5:5. Varied 50 wt% SPI-CP mixtures were prepared and hydrated at 4 °C for at least 24 h. Approximately 4g was placed in a closed chamber between two plastic films. Sealing the cones prevents water evaporation at high temperatures so that a cavity pressure of 4.5 MPa can be achieved. Mechanical treatment was provided by the oscillatory movement of the lower cone and can be adjusted by varying the angular frequency ω and strain γ. First, an oscillation time sweep experiment was conducted at a high frequency (10 Hz) and strain (80%) for 15 min at 140 °C. Second, a temperature sweep experiment (10Hz, 80%) was performed from 40 °C to 140 °C at a heating rate of 10 °C/min, and then the temperature was held at 140 °C for 5 min, followed by cooling at 4 °C/min.

2.4. Preparation of high-moisture extrudates

The protein mixtures were prepared by mixing SPI and CP with weight ratios of 10:0, 9:1, 8:2, 7:3, 6:4, 5:5. The SPI and CP had a similar size, suggesting that they can be mixed evenly. A twin-screw extruder with co-rotating design (Lab-20, Useon Extrusion, China) was used to prepare the high-moisture extrudates. The screws were with a 15.5-mm screw diameter and a 25 length-to-diameter ratio. The extruder borrel was divided into 7 separately heated and thermally controlled zones. A water pump was employed to introduce water into the extruder. Based on preliminary experiments, the extrusion conditions were set as follows: a feed moisture content of 300 g/h (50 wt% moisture), the screw speed of 180 r/min, and the extruder barrel temperatures of 25 °C,

40 °C, 60 °C, 90 °C, 130 °C, 140 °C, and 110 °C along the extruding direction. The end of the extruder was fitted with a cooling die with dimensions of 20 × 5 × 240 mm (H × W × L) and was maintained at 75 °C by running water. During steady-state operating conditions, extrudates were collected and stored in polyethylene bags in a freezer (−18 °C) before further analysis.

2.5. Tensile strength analysis

A texture analyser (TA.XT2, Stable Micro Systems, Ltd., Godalming, UK) was used with a load cell of 100 N. A dog bone-shaped mold was used to cut extrudates in parallel or perpendicular to the extrusion direction. The samples were approximately 12.0 mm in length, 3.2 mm in width, and its thickness were measured to calculate the cross-sectional area (A_0). The test was conducted at room temperature with a displacement rate of 1 mm/s. Abrasive paper was used to prevent slipping during testing when the samples were placed between two sand-coated clamps. A stress–strain curve was used to determine tensile stress and tensile strain at rupture. The tensile stress (σ, Pa) and tensile strain (ε, −) are defined as follows:

$$\varepsilon_h = \ln\frac{h(t)}{h_0}\ [-] \tag{3}$$

$$A(t) = \frac{h(t)}{h_0} \bullet A_0\ [\mathrm{m}^2] \tag{4}$$

$$\sigma(t) = \frac{F(t)}{A(t)}\ [\mathrm{Pa}] \tag{5}$$

where h_0 is the length of the sample (e.g., 12.0 mm), $h(t)$ is the length over time t, $A(t)$ is the cross-sectional area of the bar, A_0 is the area of the initial contact surface, and $F(t)$ is the force per unit area of $A(t)$. The fracture stress or fracture strain is at the point where there is a dramatic decrease in stress. For each sample, a total of 9 specimens in parallel and perpendicular directions were collected. The ratio of the averaged values measured in the parallel and perpendicular directions was used as an indication of the mechanical anisotropy (AI) of the samples.

2.6. Confocal scanning laser microscopy

A confocal laser scanning microscope was used to visualize the microstructures of the extrudates. The samples were cut in parallel and perpendicular to the direction of extrusion (approximately 20 mm) and then rapidly pre-frozen with a freeze embedding agent (Tissue-Tek O.C.T Compound, Sakura Finetek, Torrance, CA) at −20 °C. Subsequently, the samples were placed on a tray and sectioned with a cryo-microtome (CM1950, Leica, Germany) at −20 °C, yielding sliced approximately 20 μm thick in a regular pattern. A mixture of Rhodamine B (0.2 mg/mL in 75% ethanol) and Calcofluor white stain (0.05% v/v in 75% ethanol) solution was added to stain the protein and chitin, respectively. The sample was observed with laser wavelength excitations of 405 nm (for Calcofluor white) and 552 nm (for Rhodamine B) using a TCS SP8 confocal laser scanning microscope (Leica, Germany) with an HC PL APO 10 × /0.4 CS lens. Using panoramic scanning mode to capture sliced samples. At least 6 images were analyzed for each sample.

2.7. GC/O/MS analysis

GC/O/MS analysis was performed using a GC/MS-QP2020NX system (Shi-madzu, Kyoto, Japan) equipped with an SH-WAX column (30 m × 0.25 mm × 0.25 μm; Shimadzu, Kyoto, Japan) following the method described by Xu et al. (2024). The GC was operated in splitless mode, and the injection ports was held to 250 °C for 7 min. Helium, at a flow rate of 1.8 mL/min, was used as the carrier gas. The oven temperature program started at 40 °C for 0.5 min, then increased to 100 °C at 5 °C/min, and finally raised to 230 °C at 10 °C/min for 5 min. The output from the capillary column was split 1:1 (v/v) between the MS and the olfactometer (ODE-2030, Shimadzu, Kyoto, Japan). For MS, the ion source was set to 200 °C and the interface to 250 °C. Full scan mode was used, ranging from 33 to 400 m/z under electron-impact (EI) ionization at 70 eV. The transfer line for the olfactometer was kept at 200 °C, and moist air was supplied to the sniffing port at 40 mL/min to prevent dryness. Flavour compounds were identified and described by assessors, with intensity and description recorded using ODE-2030 software (Shimadzu, Kyoto, Japan).

Three trained GC/O assessors (two males, one female) participated in the analysis. They described the flavor characteristics, intensity, and pleasantness of the detected compounds, following two weeks of training. The panel used Odor Specific Magnitude Estimation (OSME) to evaluate the perceived intensity of flavours on a scale from 0 to 5, with increasing values indicating stronger intensity. Each sample was sniffed twice by the assessors, and the training process was adapted from the literature with some modifications (Gu et al., 2022). The intensities of the odor extracts were recorded by the panel, with three experienced panel members required to sniff each sample twice.

2.8. Statistical analysis

All measurements were carried out in triplicate unless otherwise specified. Analyses were conducted using Statisticix version 9.0 (Analytical Software, Tallahassee, FL). ANOVA with the least significant difference and 95% confidence interval was used to compare the means.

3. Results and discussion

3.1. Physicochemical properties of CP

The physicochemical properties of cricket powder (CP) are summarized in Table 1. The protein content of CP was 72.10 ± 0.61%, which was estimated using a nitrogen-to-protein conversion factor of 6.25. This value could be overestimated due to the presence of nitrogen from chitin, a main component of cricket exoskeletons, which also contributes nitrogen (Janssen et al., 2017; Jonas-Levi and Martinez, 2017). CP contained 31.6 ± 1.54% lipid, which was slightly higher than reported in other studies (da Rosa Machado and Thys, 2019; Montowska et al., 2019). The lipid content in insects can vary depending on factors such as sex, life stage and diet (Tzompa-Sosa et al., 2014). The dietary fiber content included 8.55 ± 1.56% soluble fiber and 24.6 ± 1.45% insoluble fiber, primarily derived from exoskeletons.

The solubility of CP was 31.25 ± 0.97%, consistent with values obtained in other studies (Perez-Fajardo et al., 2023; Stone et al., 2019). The water holding capacity (WHC) of CP was 1.08 ± 0.01 (g/g), which was relatively lower than published values of 1.76 g/g or 2.87 g/g (da Rosa Machado and Thys, 2019; Stone et al., 2019). This lower WHC could be attributed to severe thermal treatment during the dehydration process, which can induce protein denaturation and expose hydrophobic groups, thereby affecting the ability of powder to absorb water (Zhao et al., 2020).

Table 1
Physicochemical properties of cricket powder (CP).

Properties	CP
Protein content (including chitin nitrogen)	72.10 ± 0.61%
Moisture content	4.09 ± 0.22%
Lipid content	31.6 ± 1.54%
Insoluble fiber	24.60 ± 1.45%
Soluble fiber	8.55 ± 4.46%
Soluble protein	7.86 ± 0.16%
Solubility	31.25 ± 0.97%
Water holding capacity	1.08 ± 0.01 (g/g)

* Data obtained from product specification of manufacturer.

3.2. Rheological properties of SPI-CP blends

Fig. 1A illustrates the complex modulus (G^*) of SPI-CP blends with varying weight ratios, subjected to high frequency and strain (10 Hz, 80%) in a closed cavity rheometer at 140 °C. In the absence of CP, the G^* of SPI decreased over time. This trend aligns with our previous research on SPI with large soluble aggregates, suggesting that the SPI protein degradation exceeded protein aggregation at 140 °C (Deng et al., 2023; Fu et al., 2023). The G^* curves of SPI-CP blends exhibited a similar pattern, but the addition of CP accelerated the reduction in G^* values, likely due to the degradation of highly denatured cricket protein or the lubrication effect of lipids (Cheftel et al., 1992). These results indicate that the rheological properties of SPI-CP are time-dependent.

Fig. 1B shows dynamic rheological changes of SPI-CP blends during heating (40–140 °C), isothermal (140 °C), and cooling processes (140–80 °C). The G^* of SPI-CP blends decreased as the temperature increased during the heating process. The decrease in G^* slowed between 70 and 100 °C for blends containing 0–30% CP, likely due to ongoing protein aggregation and degradation reactions. With higher CP additions, the G^* decreased rapidly without slowing, suggesting that protein aggregation decreased while degradation increased. During the cooling process, the G^* increased as the temperatures decreased. For blends without CP or with 10% CP, the G^* values at the end of the cooling process (80 °C) were similar to those at 80 °C during the heating process. However, for blends with higher CP additions (20–50%), the G^* values during the cooling process were much lower than those during the heating process, likely attributed to a macroscopic separation caused by insoluble fractions and lipid from CP. A similar phenomenon was observed in SPI blends with insoluble dietary fibre and in calcium caseinate dispersions with fat, where a high proportion of insoluble components or fat induced macroscopic separation that disrupted the protein continuous structure (Deng et al., 2023; Manski et al., 2008).

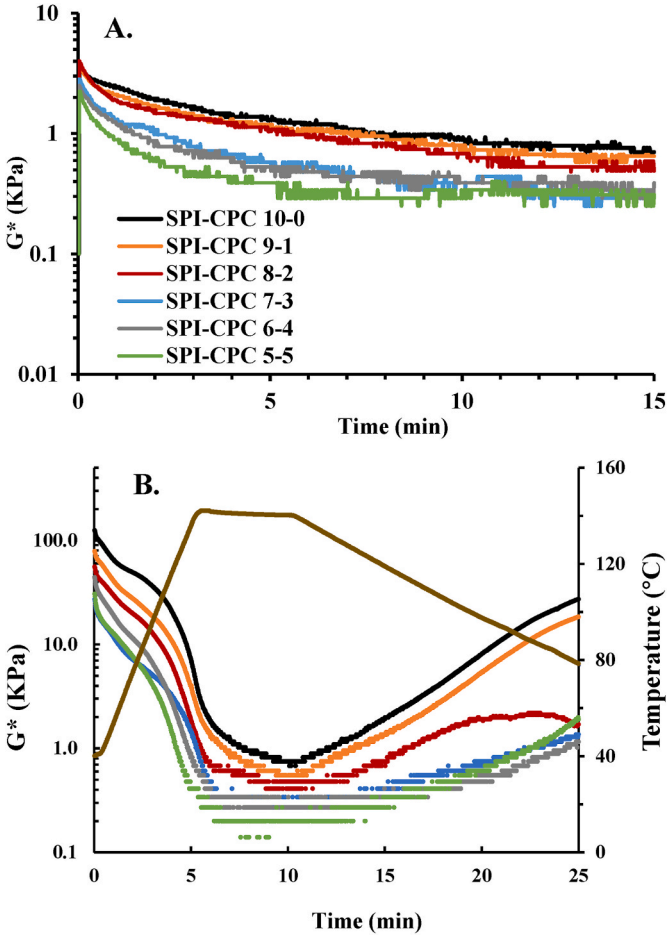

Fig. 1. A) Time sweep measurements (80%, 10 Hz) at 140 °C and B) temperature sweep measurements during heating (40–140 °C), isothermal (140 °C), and cooling processes (140–80 °C) for SPI-CP blends with weight ratios of 10:0, 9:1, 8:2, 7:3, 6:4 and 5:5.

3.3. Structural properties of extrudates

The macrostructure of SPI-CP extrudates is shown in Fig. 2. Their morphology was examined by manually deforming the samples. Without CP, the SPI extrudate showed a homogeneous gel-like structure without distinct layers or fibers. When 10% of the SPI was replaced with CP, the extrudate formed layers aligned along the extrusion flow direction. At 20% CP content, a layered structure formed perpendicular to the extrusion flow direction. When the CP content was increased to 30%, the structure exhibited layered clusters when manually deformed. With further CP additions (40% and 50%), the extrudates exhibited a disordered or damaged structure.

When the SPI-CP ratio was fixed at 9:1, the influence of varying moisture content on macrostructure is shown in Fig. 2B. At 60 wt% moisture, the extrudate had a soft texture and a disordered structure. As moisture content decreased to 55 wt% and 50 wt%, the extrudates developed layered structures in different orientations. The extrudate with 55 wt% moisture showed layers perpendicular to the extrusion flow direction. At 45 wt% moisture, the extrudates exhibited a harder texture and either a disordered structure or layers perpendicular to flow direction. Overall, the SPI-CP blend with a 9:1 ratio and 50 wt% moisture content produced the most anisotropic structure.

The mesostructure of SPI-CP extrudates with different ratios of CP addition is shown in Fig. 3. The protein appears red after labeling with Rhodamine B, while cricket fragments containing chitin appear blue or grey after labeling with Calcofluor white. The extrudate without CP consisted primarily of protein, which Calcofluor white cannot stain. CP with chitin was dispersed in the protein matrix, and their area fraction increased with increasing CP addition. These images also showed cracks, indicating week spots that were easily damaged during cryosectioning. The extrudates with 10% CP displayed a V-shape laminar structure. When the CP content was increased to 20% and 30%, the structure with filaments became more disordered. Higher CP additions (40% and 50%) resulted in a crumbled structure without filaments. Overall, low concentrations of CP (10–20%) in extrudates acted as dispersed phase and enhanced filament formation, while high concentrations of CP (30–50%) damaged the structural integrity.

3.4. Tensile properties of extrudates

The macrostructure and mesostructured of extrudate revealed that the addition of CP to SPI enhanced anisotropic structure formation (Figs. 2 and 3). To evaluate the mechanical strength and anisotropy of the extrudates, fracture stress (σ) and strain (ε) were measured in both parallel and perpendicular directions (Fig. 4). In the absence of CP, the SPI extrudate showed little anisotropy, with an anisotropic index (AI) of 1.1 for σ and 0.8 for ε, consistent with its homogenous macrostructure (Fig. 1). Replacing 10% SPI with CP, increased the AI of σ to 1.4 and ε to 1.1.

When 20% CP was added, the AI of σ and ε decreased to 0.8 and 1.2, respectively, and the σ value decreased significantly in both parallel and perpendicular direction compared to the extrudate with 10% CP. This trend aligned with findings by Smetana et al. (2018a). who reported that a significant reduction in the shear force of extrudates with increased cricket protein in both parallel and perpendicular directions to extrusion. These reduced values suggested that adding CP diminished the cohesion of extrudates due to the presence of insoluble components in CP. With 30% CP addition, the AI of σ and ε further decreased to 0.7 for both, which was attributed to higher σ and ε values in the perpendicular

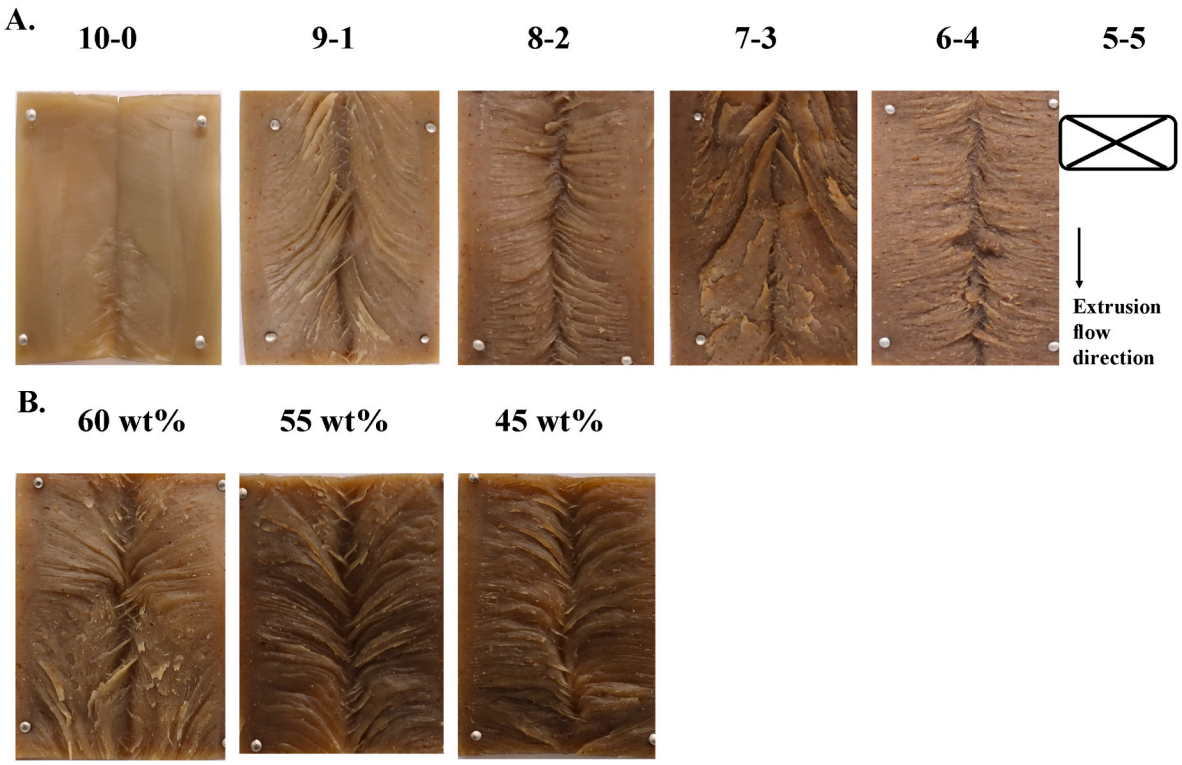

Fig. 2. Macrostructure of SPI-CP extrudates: A) Extrudates with 50 wt% moisture and varying CP content (SPI-CP ratios of 10:0, 9:1, 8:2, 7:3, 6:4 and 5:5); B) Extrudates with 10% CP and varying moisture content (60 wt%, 55 wt%, 50 wt% and 45 wt%).

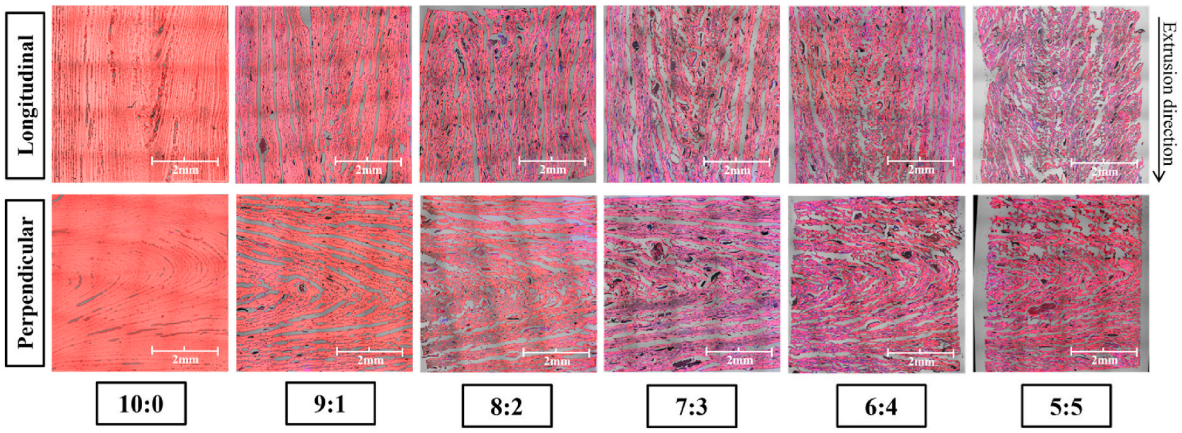

Fig. 3. CLSM images of SPI-CP extrudates with weight ratios of 10:0, 9:1, 8:2, 7:3, 6:4 and 5:5. Red indicates protein; blue/grey indicates cricket fragments with chitin. This perpendicular direction is the edge of the extrusion die.

direction compared to the parallel direction. Similar trends were observed in extrudates with 60 wt%, 55 wt% and 45 wt% moisture (data shown in Fig. S1), which correlated with the observation of the layers orientation seen in Fig. 2B. For the extrudate with 40% CP, no significant anisotropy in σ and ε was noted, and the extrudate with 50% CP lacked sufficient coherence for tensile testing. These changes in mechanical anisotropy at CP levels above 10% were consistent with the morphological observation (Figs. 2 and 3), likely linked to macroscopic separation due to the insoluble fraction and lipid present in CP.

3.5. Flavor compounds in extrudates

Flavor compounds and their intensities in SPI and SPI-CP extrudates (SPI-CP ratio of 9:1) were analyzed using GC/O/MS (Table 2). Fourteen flavor compounds were identified in the SPI extrudates, including aldehydes (n = 5), alcohols (n = 3), ketones (n = 3), a furan (n = 1), a hydrocarbon (n = 1), and a thiophenes (n = 1). Thirteen flavor compounds were identified in the SPI-CP extrudates, consisting of aldehydes (n = 6), an alcohol (n = 1), pyrazines (n = 2), ethers (n = 2), a furan (n = 1), and a phenol (n = 1). The SPI extrudates contained aldehydes, alcohols and thiophene, contributed to a stronger green and astringent flavor, leading to a beany or off-flavor. With the addition of CP, more pyrazines and ethers were detected, giving the extrudate a burnt and baked flavor. Moreover, the lipids in CP led to the formation of intermediate lipid oxidation products, such as benzaldehyde and 4-ethylbenzaldehyde. Therefore, adding antioxidants during extrusion could be recommended for future applications to not only improve the flavor profile but also enhance the storage stability of meat analogs (Yuan et al., 2023).

CP has garnered increasing attention not only for its high nutritional

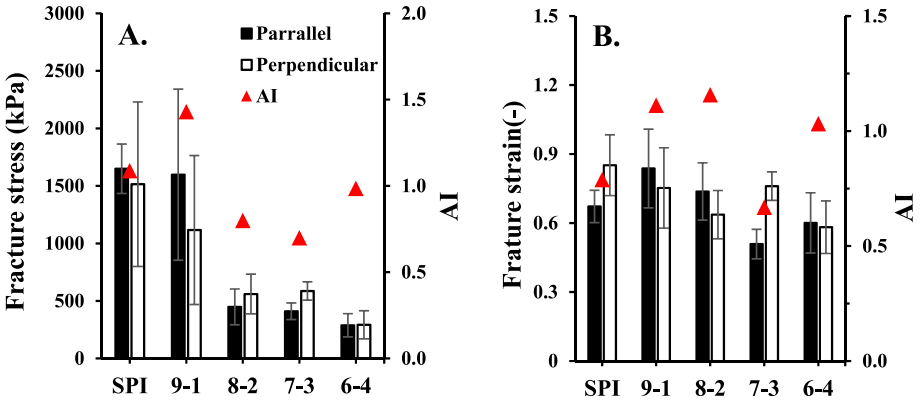

Fig. 4. A) Fracture stress and B) fracture strain of SPI-CP extrudates deformed in parallel and perpendicular directions. The ratio of the averaged values measured in the parallel and perpendicular directions was used as an indication of the mechanical anisotropy (AI) of the samples.

Table 2
Flavor compounds and intensity in extrudates.

Compounds	Odor description	Chemical classification	Odor intensity of extrudates	
			SPI	SPI-CP (9:1)
Hexanal	Grassy aroma	Aldehydes	2.66	2.33
Octanal	Lemon scent		3	ns
2-Hexenal, 2-ethyl-	Steamed aroma		4	3.67
Nonanal	Lemon scent		4.33	ns
2-Octenal, (E)-	Fatty taste		3	3.33
Benzaldehyde, 4-ethyl-	Fatty taste		ns	3
2-n-Butylacrolein	Spicy aroma		ns	3.67
Benzaldehyde	Almond aroma		ns	2
1-Adamantanol	Mushroom fragrance	Alcohols	3	2.67
1-Octen-3-ol	Moldy taste		4.33	ns
n-Heptadecanol-1	Waxy taste		3	ns
2-Cyclopenten-1-one, 2,3-dimethyl-	Roasted aroma	Ketones	3.33	ns
trans-3-Nonen-2-one	Unripe taste		4	ns
Ethanone, 1-(3-butyloxiranyl)-	Floral aroma		2.67	ns
Pyrazine, trimethyl-	Bean fragrance	Pyrazines	ns	2.33
Pyrazine, 3-ethyl-2,5-dimethyl-	Toasted fragrance		ns	5
Allyl n-octyl ether	Sweet fragrance	Ethers	ns	2.67
Benzeneacetic acid 1-methylethyl ester	Sweet fragrance		ns	3.67
Furan, 2-pentyl-	Roasted flavour	Furans	2.33	2.67
4-[[3-(3,5-Dimethyl-pyrazol-1-yl)-[1,2,4]triazol-4-ylimino]methyl]-2-ethoxy-phenol	Spicy aroma	Phenols	ns	3
Heneicosane	Waxy taste	Hydrocarbons	2	ns
Thiophene, 2-pentyl-	Bean odor	Thiophenes	3.33	ns

content but also for its influence on the sensory attributes of food products (Carrera et al., 2018). The incorporation of CP in formulations significantly impacts taste and flavor, due to the presence of flavor-active compounds such as pyrazines and ethers (Kröger et al., 2022). These compounds contribute to roasted, nutty, and earthy aromas, enhancing the sensory appeal of protein-based extrudates. For example, pyrazines develop via the Maillard reaction during high-temperature processes like extrusion, resulting in desirable toasted and savory flavor notes (Sun et al., 2022). These flavor characteristics are especially beneficial for improving the taste of SPI extrudates, which are often considered bland or unappealing (Yılmaz and Gökmen, 2017).

However, while cricket protein introduces complex and favorable flavors, its effect on taste must be carefully controlled. Higher concentrations of CP can lead to the development of bitter or metallic notes, which may negatively affect the overall sensory experience. Research indicates that the optimal flavor enhancement occurs when CP is included at approximately 10% in SPI-based extrudates. At this concentration, the desirable roasted and baked flavors from CP are maximized without introducing off-flavors or compromising the structural integrity of the product. Above this threshold, insoluble components in CP may cause sensory defects, such as overly earthy or bitter tastes, potentially reducing consumer acceptance. Thus, precise optimization of CP levels is critical for achieving a balance between flavor enhancement and overall product quality.

4. Conclusion

The addition of CP enhances anisotropic structure formation, with varying effects on structural and mechanical properties depending on the CP concentration. Lower concentration of CP (10%) improved structural and mechanical anisotropy, whereas higher concentrations (20–50%) reduced mechanical strength and coherence, primarily due to insoluble components and large crack formation. In terms of flavor, the addition of CP introduced more pyrazines and ethers, contributing to a desirable burnt and baked flavor profile. These findings indicated that CP could enhance the textural properties of SPI-based meat analogs. Further optimization of processing technology, including dehydration and purification, incorporation levels in SPI blends and extrusion processing conditions are essential to balance its addition and maximized its benefits in improving the textural and mechanical properties of SPI-based extrudates.

CRediT authorship contribution statement

Zhaojun Wang: Writing – original draft, Methodology, Formal analysis. **Qian Deng:** Experimental work, Investigation, Data curation, Formal analysis, Visualization, Writing – original draft. **Yuliang Zhou:** Experimental work. **Xinyue Qi:** Data curation, and proofreading. **Lee-how Lau:** Writing and Proofreading. **Yuqiao He:** Formal analysis, and Figure organization. **Zhiyong He:** Resources. **Maomao Zeng:** Resources. **Qiuming Chen:** Resources. **Jie Chen:** Resources. **Hui Ye:** Writing – review & editing, Conceptualization, Supervision.

Funding data availability

This work was supported by grants from the National Natural Science Foundation of China (grant number 32202081) to ZW; Ministry of Education, Singapore AcRF Tier 1 Seed Funding Grant (RS10/23) and AcRF Tier 1 Grant (RG90/23) to HY; NTU-Research Scholarship R2301921 to XQ.

Declaration of Competing Interest

None.

Data availability

Data will be made available on request.

References

Alcorta, A., Porta, A., Tárrega, A., Alvarez, M.D., Vaquero, M.P., 2021. Foods for plant-based diets: challenges and innovations. Foods 10 (2), 293. https://doi.org/10.3390/foods10020293.

Carrera, M., Cañas, B., Gallardo, J.M., 2018. Advanced proteomics and systems biology applied to study food allergy. Curr. Opin. Food Sci. 22, 9–16.

Cheftel, J.C., Kitagawa, M., Queguiner, C., 1992. New protein texturization processes by extrusion cooking at high moisture levels. In: Food Reviews International, pp. 235–275. https://doi.org/10.1080/87559129209540940, 8, Issue 2.

Chirico Scheele, S., Hoque, M.N., Christopher, G., Egan, P.F., 2021. Printability and fidelity of protein-enriched 3D printed foods: a case study using cricket and pea protein powder. In: International Design Engineering Technical Conferences and Computers and Information in Engineering Conference, vol. 85413. https://doi.org/10.1115/DETC2021-67783. V005T05A001.

Dekkers, B.L., Nikiforidis, C.V., van der Goot, A.J., 2016. Shear-induced fibrous structure formation from a pectin/SPI blend. Innovative Food Sci. Emerging Technol. 36, 193–200. https://doi.org/10.1016/j.ifset.2016.07.003.

Dekkers, B.L., Boom, R.M., van der Goot, A.J., 2018a. Viscoelastic properties of soy protein isolate - pectin blends: richer than those of a simple composite material. Food Res. Int. 107, 281–288. https://doi.org/10.1016/j.foodres.2018.02.037.

Dekkers, B.L., Emin, M.A., Boom, R.M., van der Goot, A.J., 2018b. The phase properties of soy protein and wheat gluten in a blend for fibrous structure formation. Food Hydrocolloids 79, 273–281. https://doi.org/10.1016/j.foodhyd.2017.12.033.

Deng, Q., Wang, Z., Fu, L., He, Z., Zeng, M., Qin, F., Chen, J., 2023. High-moisture extrusion of soy protein: effects of insoluble dietary fiber on anisotropic extrudates. Food Hydrocolloids 141 (March), 108688. https://doi.org/10.1016/j.foodhyd.2023.108688.

Fu, L., Wang, Z., He, Z., Zeng, M., Qin, F., Chen, J., 2023. Effects of soluble aggregates sizes on rheological properties of soybean protein isolate under high temperature. LWT 182, 114793. https://doi.org/10.1016/j.lwt.2023.114793.

Fu, L., Wang, Z., Adhikari, B., He, Z., Zeng, M., Qin, F., Chen, J., 2024. Soluble and insoluble fractions of soy protein isolate affect the properties of its high-moisture extrudates. Food Biosci. 59, 103850. https://doi.org/10.1016/j.fbio.2024.103850.

Gómez, B., Munekata, P.E.S., Zhu, Z., Barba, F.J., Toldrá, F., Putnik, P., Kovačević, D.B., Lorenzo, J.M., 2019. Challenges and opportunities regarding the use of alternative protein sources: aquaculture and insects. Adv. Food Nutr. Res. 89, 259–295. https://doi.org/10.1016/bs.afnr.2019.03.003.

Grabowska, K.J., Tekidou, S., Boom, R.M., van der Goot, A.J., 2014. Shear structuring as a new method to make anisotropic structures from soy–gluten blends. Food Res. Int. 64, 743–751. https://doi.org/10.1016/J.FOODRES.2014.08.010.

Gu, Z., Jin, Z., Schwarz, P., Rao, J., Chen, B., 2022. Uncovering aroma boundary compositions of barley malts by untargeted and targeted flavoromics with HS-SPME-GC-MS/olfactometry. Food Chem. 394, 133541. https://doi.org/10.1016/j.foodchem.2022.133541.

Halloran, A., Roos, N., Eilenberg, J., Cerutti, A., Bruun, S., 2016. Life cycle assessment of edible insects for food protein: a review. Agron. Sustain. Dev. 36, 1–13. https://doi.org/10.1007/s13593-016-0392-8.

Van Huis, A., 2013. Potential of insects as food and feed in assuring food security. Annu. Rev. Entomol. 58, 563–583. https://doi.org/10.1146/annurev-ento-120811-15370.

Janssen, R.H., Vincken, J.-P., van den Broek, L.A.M., Fogliano, V., Lakemond, C.M.M., 2017. Nitrogen-to-protein conversion factors for three edible insects: Tenebrio molitor, Alphitobius diaperinus, and Hermetia illucens. J. Agric. Food Chem. 65 (11), 2275–2278. https://doi.org/10.1021/acs.jafc.7b00471.

Jonas-Levi, A., Martinez, J.-J.I., 2017. The high level of protein content reported in insects for food and feed is overestimated. J. Food Compos. Anal. 62, 184–188. https://doi.org/10.1016/j.jfca.2017.06.004.

Kiiru, S.M., Kinyuru, J.N., Kiage, B.N., Martin, A., Marel, A., Osen, R., 2020. Extrusion texturization of cricket flour and soy protein isolate: influence of insect content, extrusion temperature, and moisture-level variation on textural properties. Food Sci. Nutr. 8 (8), 4112–4120. https://doi.org/10.1002/fsn3.1700.

Kröger, T., Dupont, J., Büsing, L., Fiebelkorn, F., 2022. Acceptance of insect-based food products in western societies: a systematic review. Front. Nutr. 8, 759885.

Lamsal, B., Wang, H., Pinsirodom, P., Dossey, A.T., 2019. Applications of insect-derived protein ingredients in food and feed industry. JAOCS (J. Am. Oil Chem. Soc.) 96 (2), 105–123. https://doi.org/10.1002/aocs.12180.

Manski, J.M., van der Goot, A.J., Boom, R.M., 2007. Formation of fibrous materials from dense calcium caseinate dispersions. Biomacromolecules 8 (4), 1271–1279. https://doi.org/10.1021/bm061008p.

Manski, J.M., van der Zalm, E.E., van der Goot, A.J., Boom, R.M., 2008. Influence of process parameters on formation of fibrous materials from dense calcium caseinate dispersions and fat. Food Hydrocolloids 22 (4), 587–600. https://doi.org/10.1016/j.foodhyd.2007.02.006.

Montowska, M., Kowalczewski, P.Ł., Rybicka, I., Fornal, E., 2019. Nutritional value, protein and peptide composition of edible cricket powders. Food Chem. 289, 130–138. https://doi.org/10.1016/j.foodchem.2019.03.062.

Nieuwland, M., Heijnis, W., van der Goot, A.-J., Hamoen, R., 2023. XRT for visualizing microstructure of extruded meat replacers. Curr. Res. Food Sci. 6, 100457. https://doi.org/10.1016/j.crfs.2023.100457.

Oonincx, D.G.A.B., De Boer, I.J.M., 2012. Environmental impact of the production of mealworms as a protein source for humans–a life cycle assessment. PLoS One 7 (12), e51145. https://doi.org/10.1371/journal.pone.0051145.

Osimani, A., Milanović, V., Cardinali, F., Roncolini, A., Garofalo, C., Clementi, F., Pasquini, M., Mozzon, M., Foligni, R., Raffaelli, N., 2018. Bread enriched with cricket powder (Acheta domesticus): a technological, microbiological and nutritional evaluation. Innovat. Food Sci. Emerg. Technol. 48, 150–163. https://doi.org/10.1016/j.ifset.2018.06.007.

Pauter, P., Różańska, M., Wiza, P., Dworczak, S., Grobelna, N., Sarbak, P., Kowalczewski, P., 2018. Effects of the replacement of wheat flour with cricket powder on the characteristics of muffins. Acta Scientiarum Polonorum Technologia Alimentaria 17 (3), 227–233. https://doi.org/10.17306/J.AFS.2018.0570.

Perez-Fajardo, M., Bean, S.R., Ioerger, B., Tilley, M., Dogan, H., 2023. Characterization of commercial cricket protein powder and impact of cricket protein powder replacement on wheat dough protein composition. Cereal Chem. 100 (3), 574–586. https://doi.org/10.1002/cche.10658.

Pilco-Romero, G., Chisaguano-Tonato, A.M., Herrera-Fontana, M.E., Chimbo-Gándara, L. F., Sharifi-Rad, M., Giampieri, F., Battino, M., Vernaza, M.G., Álvarez-Suárez, J.M., 2023. House cricket (Acheta domesticus): a review based on its nutritional composition, quality, and potential uses in the food industry. Trends Food Sci. Technol. 104226. https://doi.org/10.1016/j.tifs.2023.104226.

da Rosa Machado, C., Thys, R.C.S., 2019. Cricket powder (Gryllus assimilis) as a new alternative protein source for gluten-free breads. Innovat. Food Sci. Emerg. Technol. 56, 102180. https://doi.org/10.1016/j.ifset.2019.102180.

Rumpold, B.A., Schlüter, O.K., 2013. Nutritional composition and safety aspects of edible insects. Mol. Nutr. Food Res. 57 (5), 802–823. https://doi.org/10.1002/mnfr.201200735.

Schreuders, F.K.G., Schlangen, M., Bodnár, I., Erni, P., Boom, R.M., van der Goot, A.J., 2022. Structure formation and non-linear rheology of blends of plant proteins with pectin and cellulose. Food Hydrocolloids 124, 107327. https://doi.org/10.1016/j.foodhyd.2021.107327.

van der Sman, R.G.M., van der Goot, A.J., 2023. Hypotheses concerning structuring of extruded meat analogs. Curr. Res. Food Sci. 6 (April), 100510. https://doi.org/10.1016/j.crfs.2023.100510.

Smetana, S., Larki, N.A., Pernutz, C., Franke, K., Bindrich, U., Toepfl, S., Heinz, V., 2018a. Structure design of insect-based meat analogs with high-moisture extrusion. J. Food Eng. 229, 83–85. https://doi.org/10.1016/j.jfoodeng.2017.06.035.

Smetana, S., Pernutz, C., Toepfl, S., Heinz, V., Van Campenhout, L., 2018b. High-moisture extrusion with insect and soy protein concentrates: cutting properties of meat analogues under insect content and barrel temperature variations, 5(1), 29–34. https://doi.org/10.3920/JIFF2017.0066.

Stone, A.K., Tanaka, T., Nickerson, M.T., 2019. Protein quality and physicochemical properties of commercial cricket and mealworm powders. J. Food Sci. Technol. 56, 3355–3363. https://doi.org/10.1007/s13197-019-03818-2.

Sun, A., Wu, W., Soladoye, O.P., Aluko, R.E., Bak, K.H., Fu, Y., Zhang, Y., 2022. Maillard reaction of food-derived peptides as a potential route to generate meat flavor compounds: a review. Food Res. Int. 151, 110823.

Terry, P., Lupul, M., Coate, K., 2017. Evaluating the protein content in chocolate chip cookies using cricket powder as a flour replacement. J. Acad. Nutr. Diet. 117 (9), A56.

Tzompa-Sosa, D.A., Yi, L., van Valenberg, H.J.F., van Boekel, M.A.J.S., Lakemond, C.M. M., 2014. Insect lipid profile: aqueous versus organic solvent-based extraction methods. Food Res. Int. 62, 1087–1094. https://doi.org/10.1016/j.foodres.2014.05.052.

Wang, Z., Dekkers, B.L., Boom, R., van der Goot, A.J., 2019a. Maltodextrin promotes calcium caseinate fibre formation through air inclusion. Food Hydrocolloids 95, 143–151. https://doi.org/10.1016/j.foodhyd.2019.04.028.

Wang, Z., Tian, B., Boom, R., van der Goot, A.J., 2019b. Air bubbles in calcium caseinate fibrous material enhances anisotropy. Food Hydrocolloids 87 (May 2018), 497–505. https://doi.org/10.1016/j.foodhyd.2018.08.037.

Wang, Z., Ji, Y., Fu, L., Pan, H., He, Z., Zeng, M., Qin, F., Chen, J., 2023. Potential use of gluten hydrolysate as a plasticizer in high-moisture soy protein–gluten extrudates. J. Food Eng. 354, 111565. https://doi.org/10.1016/j.jfoodeng.2023.111565.

Wittek, P., Zeiler, N., Karbstein, H.P., Emin, M.A., 2021. High moisture extrusion of soy protein: investigations on the formation of anisotropic product structure. Foods 10 (102). https://doi.org/10.3390/foods10010102.

Xiao, X., Zou, P.-R., Hu, F., Zhu, W., Wei, Z.-J., 2023. Updates on plant-based protein products as an alternative to animal protein: technology, properties, and their health benefits. Molecules 28 (10), 4016. https://doi.org/10.3390/molecules28104016.

Xie, S., Wang, Z., He, Z.-Y., Zeng, M.-M., Fang, Q.I.N., Adhikari, B., Jie, C., 2023. The effects of maltodextrin/starch in soy protein isolate–wheat gluten on the thermal stability of high-moisture extrudates. J. Integr. Agric. 22 (5), 1590–1602. https://doi.org/10.1016/j.jia.2023.04.013.

Xu, J., Chen, Q., Zeng, M., Qin, F., Chen, J., Zhang, W., Wang, Z., He, Z., 2024. Effect of heat treatment on the release of off-flavor compounds in soy protein isolate. Food Chem. 437, 137924. https://doi.org/10.1016/j.foodchem.2023.137924.

Yi, L., Lakemond, C.M.M., Sagis, L.M.C., Eisner-Schadler, V., Van Huis, A., van Boekel, M. A.J.S., 2013. Extraction and characterisation of protein fractions from five insect species. Food Chem. 141 (4), 3341–3348. https://doi.org/10.1016/j.foodchem.2013.05.115.

Yılmaz, C., Gökmen, V., 2017. Formation of tyramine in yoghurt during fermentation–Interaction between yoghurt starter bacteria and Lactobacillus plantarum. Food Res. Int. 97, 288–295.

Yuan, J., Qin, F., He, Z., Zeng, M., Wang, Z., Chen, J., 2023. Influences of spices on the flavor of meat analogs and their potential pathways. Foods 12 (8), 1650. https://doi.org/10.3390/foods12081650.

Zhao, X., Cheng, M., Zhang, X., Li, X., Chen, D., Qin, Y., Wang, J., Wang, C., 2020. The effect of heat treatment on the microstructure and functional properties of whey protein from goat milk. J. Dairy Sci. 103 (2), 1289–1302. https://doi.org/10.3168/jds.2019-17221.